



Optimization of the Performance of Heat Pipe Using Simulation Methods

Manu N D^a, Vinay L^b

^aPG Scholar, Dept. of Mechanical Engineering, Rajeev Institute of Technology, Hassan, India.

^bAsst. Prof, Dept. of Mechanical Engineering, Rajeev Institute of Technology, Hassan (India).

ABSTRACT

The heat pipe is one of the most efficient systems known today than any other systems which transport heat. Heat pipe performance depends on a number of factors. The objective of the current study is to optimize the thermal performance of heat pipe by varying the porosity and condenser length with the help of ANSYS CFX. Multiphase analysis is carried out to optimize the performance of heat pipe. The geometry of Heat Pipe is obtained from the previous literature, before optimization the results obtained for the taken geometry were validated with results available in the literature. Modeling and Meshing were made for different condenser length and porosity. Analysis is performed in ANSYS CFX with necessary boundary conditions and CFX solutions are obtained. Many iterations were carried out to achieve the good results by comparing with the results of the previous geometry results. From the results obtained by iteration the optimization is done for 2.4 Condenser length to Evaporator length ratio and 0.7 porosity.

Keywords - Heat Pipe, Thermal performance, Multiphase, Condenser length, Porosity.

1. INTRODUCTION

The heat pipe is a vapor-liquid phase-change device that transfers heat from a hot reservoir to a cold reservoir using capillary forces generated by a wick or porous material and a working fluid. Heat pipes are the most effective passive method of transferring heat available today. Heat pipes can transmit heat at high rates and have a very high thermal conductance. A heat pipe or heat pin is a heat-transfer device that combines the principles of both thermal conductivity and phase transition to efficiently manage the transfer of heat between two solid interfaces.

The heat transfer in a heat pipe depends on the parameters such as thermal conductivity of heat pipe wall, porosity of wick material, radius of heat pipe and length of the heat pipe. Increase of thermal conductivity of heat pipe wall, the maximum temperature of outer surface decreases and the thermal resistance of system decreases. The effective thermal conductivity of wick structure varies with varying wick porosity and thus the thermal resistance of system also varies. Increasing heat pipe radius, the heat transfer area increases which decreases the temperature difference in evaporator and condenser section. Increasing heat pipe length, the temperature difference between evaporator and condenser is constant so the thermal resistance of heat pipe remains constant but the pressure drop increases.

With the advent of high speed computers, Computational Fluid Dynamics (CFD) has become a complementary tool to experimental work and helps in design and optimization of components of advanced machines. The aim of the current research work is to apply a commercial CFD code to analyze the flow of the working fluid in the heat pipe and heat transfer taking in it. The main objective of this study is to simulate the given problem of heat pipe in CFX and multiphase analysis is carried out to optimize the performance of heat pipe.

1.1 Working Principle

A cylindrical heat pipe consists of three parts:

1. Evaporator section,
2. Adiabatic (transport) section
3. Condenser section.
 - Heat applied to evaporator section by an external source is conducted through the pipe wall and wick structure, where it vaporizes the working fluid.
 - The resulting vapor pressure drives the vapor through the adiabatic section to the condenser, where the vapor condenses and releasing its latent heat of vaporization to the provided heat sink.
 - The capillary pressure created by the wick structure, pumps the condensed fluid back to the evaporator. Therefore, the heat pipe can continuously transport the latent heat of vaporization from the evaporator to the condenser section.

- This process will continue as long as there is sufficient capillary pressure to drive the condensate back to the evaporator.

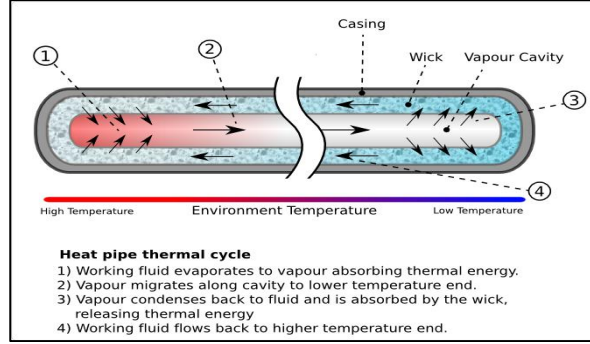


Fig 1: Mechanism for a heat pipe.

2. GOVERNING EQUATION

The governing equations in vapor region are continuity, Navier-Stokes and energy equations as following:

$$\frac{\partial u_v}{\partial x} + \frac{\partial v_v}{\partial r} + \frac{v_v}{r} = 0 \quad \dots\dots (1)$$

$$\rho_v \left(u_v \frac{\partial u_v}{\partial x} + v_v \frac{\partial u_v}{\partial r} \right) = -\frac{\partial P_v}{\partial x} + \mu_v \left[\frac{4}{3} \frac{\partial^2 u_v}{\partial x^2} + \frac{1}{r} \frac{\partial}{\partial r} \left(r \frac{\partial u_v}{\partial r} \right) + \frac{1}{r} \frac{\partial}{\partial r} \left(r \frac{\partial v_v}{\partial r} \right) - \frac{2}{3} \frac{\partial}{\partial x} \left(\frac{1}{r} \frac{\partial}{\partial r} (r v_v) \right) \right] \quad \dots\dots (2)$$

$$\rho_v \left(u_v \frac{\partial v_v}{\partial x} + v_v \frac{\partial v_v}{\partial r} \right) = -\frac{\partial P_v}{\partial r} + \mu_v \left[\frac{\partial^2 v_v}{\partial x^2} + \frac{4}{3r} \frac{\partial}{\partial r} \left(r \frac{\partial v_v}{\partial r} \right) - \frac{4}{3} \frac{v_v}{r^2} + \frac{1}{3} \frac{\partial^2 u_v}{\partial x \partial r} \right] \quad \dots\dots (3)$$

$$\rho_v C_{p,v} \left(u_v \frac{\partial T_v}{\partial x} + v_v \frac{\partial T_v}{\partial r} \right) = \frac{k_r}{r} \left[\frac{\partial}{\partial r} \left(r \frac{\partial T_v}{\partial r} \right) + r \frac{\partial^2 T_v}{\partial x^2} \right] + v_v \frac{\partial p_v}{\partial r} + u_v \frac{\partial p_v}{\partial x} \quad \dots\dots (4)$$

The boundary conditions for vapor region are as following.
The boundary conditions at both pipe ends are:

$$v = u = 0, \frac{\partial T_v}{\partial x} = 0 \quad \dots\dots (5)$$

At pipe centerline the symmetry boundary conditions are:

$$v = 0, \frac{\partial u}{\partial r} = 0 \text{ and } \frac{\partial T}{\partial r} = 0 \quad \dots\dots (6)$$

The radial velocities at liquid-vapor interface

$$\left. \begin{aligned} v_e &= + \frac{Q_e}{2\pi R_{int} L_e \rho_v h_{fg}} \\ v_a &= 0 \\ v_c &= - \frac{Q_c}{2\pi R_{int} L_c \rho_v h_{fg}} \end{aligned} \right\} \quad \dots\dots (7)$$

The temperature at the vapor-liquid interface of the evaporator and condenser is calculated approximately using Clausius-Clapeyron equation

$$T_{int} = \frac{1}{\frac{1}{T_{v,sat}} - \frac{R}{h_{fg}} \ln \frac{P_v}{P_{v,sat}}} \quad \dots\dots (8)$$

The governing equations in wick structure are as following. The Darcy's law has been employed for momentum equation in porous media:

$$\rho_l \left(u_l \frac{\partial u_l}{\partial x} + v_l \frac{\partial u_l}{\partial r} \right) = -\frac{\partial P_l}{\partial x} + \mu_l \left[\frac{1}{r} \frac{\partial}{\partial r} \left(r \frac{\partial u_l}{\partial r} \right) + \frac{\partial^2 u_l}{\partial x^2} \right] - \frac{\mu_l \varepsilon_x u_l}{K_x} \quad \dots\dots (9)$$

$$\rho_l \left(u_l \frac{\partial v_l}{\partial x} + v_l \frac{\partial v_l}{\partial r} \right) = -\frac{\partial P_l}{\partial r} + \mu_l \left[\frac{1}{r} \frac{\partial}{\partial r} \left(r \frac{\partial v_l}{\partial r} \right) + \frac{\partial^2 v_l}{\partial x^2} \right] - \frac{\mu_l \varepsilon_r u_l}{K_r} \quad \dots\dots (10)$$

$$\rho_l c_{p,l} \left(u_l \frac{\partial T_l}{\partial x} + v_l \frac{\partial v_l}{\partial r} \right) = \frac{k_{eff}}{\varepsilon} \left[\frac{1}{r} \frac{\partial}{\partial r} \left(r \frac{\partial T_l}{\partial r} \right) + \frac{\partial^2 T_l}{\partial x^2} \right] + S \quad \dots (11)$$

For homogenous isotropic wicks, the porosity and permeability are the same in all directions, so

$$\left. \begin{aligned} \varepsilon_r = \varepsilon_x = \varepsilon \\ K_r = K_x = K \end{aligned} \right\} \quad \dots (12)$$

The effective thermal conductivity of wick structure is calculated from equation for screen wire mesh,

$$k_{eff} = \frac{k_l[(k_l+k_s)-(1-\varepsilon)(k_l-k_s)]}{[(k_l+k_s)+(1-\varepsilon)(k_l-k_s)]} \quad \dots (13)$$

The boundary conditions at both pipe ends are:

$$v = u = 0, \frac{\partial T_l}{\partial x} = 0 \quad \dots (14)$$

The radial blowing and suction velocities at liquid-vapor interface

$$\left. \begin{aligned} v_e &= -\frac{Q_e}{2\pi R_{Int} L_e \rho_v h_{fg}} \\ v_a &= 0 \\ v_c &= +\frac{Q_c}{2\pi R_{Int} L_c \rho_v h_{fg}} \end{aligned} \right\} \quad \dots (15)$$

At heat pipe wall the equation of thermal conduction was used in cylindrical coordinates:

$$k_s \left[\frac{1}{r} \frac{\partial}{\partial r} \left(r \frac{\partial T_s}{\partial r} \right) + \frac{\partial^2 T_s}{\partial x^2} \right] = 0 \quad \dots (16)$$

The boundary conditions in this region are as following:

At wall-liquid interface:

$$k_{eff} \frac{\partial T_l}{\partial r} = k_s \frac{\partial T_s}{\partial r} \quad \dots (17)$$

At both ends of heat pipe:

$$\frac{\partial T_s}{\partial x} = 0 \quad \dots (18)$$

At external surface of heat pipe:

$$\left. \begin{aligned} \text{Condenser: } \frac{\partial T_s}{\partial r} &= +\frac{Q_e}{2\pi R_{Out} L_e} \\ \text{Adiabatic: } \frac{\partial T_s}{\partial r} &= 0 \\ \text{Evaporator: } \frac{\partial T_s}{\partial r} &= -\frac{Q_c}{2\pi R_{Out} L_c} \end{aligned} \right\} \quad \dots (19)$$

3. RESULT AND DISCUSSION

In this case the porosity of the wick is changed to 0.5, 0.6, 0.7 and 0.8 for various condenser length i.e. CL/EL ratio. The temperature at the condenser side varies as the condenser length is varying. So the temperature on the condenser section is noted for each CL/EL ratio and porosity. The temperature on the evaporator section will be constant as the heat flux is maintained to be constant.

Case I: Porosity is taken as 0.5 for varying CL/EL ratio. In this case for CL/EL ratio 0.8 and 1.0 the temperature curve diverges so the solution for these two ratios is not taken. After 1.0 ratio the condenser temperature goes on decreases up to a certain ratio after that it becomes constant. The difference between evaporator temperature and condenser temperature is recorded.

Porosity	CL/EL	Evaporator Temp ⁰ C	Condenser Temp ⁰ C	ET-CT ⁰ C
0.5	0.8	101	Solution Diverges	-
	1.0	101	Solution Diverges	-
	1.2	101	90.23	10.77
	1.4	101	90.43	10.57
	1.6	101	90.82	10.18
	1.8	101	92.55	8.45
	2.0	101	94.37	6.63
	2.2	101	94.46	6.54
	2.4	101	94.53	6.47
	2.6	101	94.51	6.49
	2.8	101	94.51	6.49
	3.0	101	94.51	6.49
	3.2	101	94.51	6.49
	3.4	101	94.51	6.49

Table 1: Temperature Difference at 0.5 Porosity.

Case II: Porosity is taken as 0.6 for varying CL/EL ratio.

Porosity	CL/EL	Evaporator Temp ⁰ C	Condenser Temp ⁰ C	ET-CT ⁰ C
0.6	0.8	101	Solution Diverges	-
	1.0	101	Solution Diverges	-
	1.2	101	92.57	8.43
	1.4	101	92.68	8.32
	1.6	101	93.12	7.88
	1.8	101	94.79	6.21
	2.0	101	96.62	4.38
	2.2	101	96.71	4.29
	2.4	101	96.77	4.23
	2.6	101	96.78	4.22
	2.8	101	96.78	4.22
	3.0	101	96.78	4.22
	3.2	101	96.78	4.22
	3.4	101	96.78	4.22

Table 2: Temperature Difference at 0.6 Porosity.

CASE III: In this case the porosity is kept constant to 0.7 for the varying CL/EL ratio.

Porosity	CL/EL	Evaporator Temp ⁰ C	Condenser Temp ⁰ C	ET-CT ⁰ C
0.7	0.8	101	Solution Diverges	-
	1.0	101	95.00	6.00
	1.2	101	95.12	5.88
	1.4	101	95.25	5.75
	1.6	101	95.52	5.48
	1.8	101	97.35	3.65
	2.0	101	99.16	1.84
	2.2	101	99.23	1.77
	2.4	101	99.34	1.66
	2.6	101	99.35	1.65
	2.8	101	99.35	1.65
	3.0	101	99.35	1.65
	3.2	101	99.35	1.65
	3.4	101	99.35	1.65

Table 3: Temperature Difference at 0.7 Porosity

CASE IV: Porosity of the wick is kept 0.8 for all varying Condenser length in this case.

Porosity	CL/EL	Evaporator Temp °C	Condenser Temp °C	ET-CT °C
0.8	0.8	101	Solution Diverges	-
	1.0	101	Solution Diverges	-
	1.2	101	93.42	7.58
	1.4	101	93.53	7.47
	1.6	101	93.82	7.18
	1.8	101	95.64	5.36
	2.0	101	97.46	3.54
	2.2	101	97.49	3.51
	2.4	101	97.59	3.41
	2.6	101	97.61	3.39
	2.8	101	97.61	3.39
	3.0	101	97.61	3.39
	3.2	101	97.61	3.39
3.4	101	97.61	3.39	

Table 4: Temperature Difference at 0.8 Porosity.

From Fig 3, it is observed that the temperature difference (dT) will decrease upto a certain CL/EL ratio and after that there will be no change in dT. For all the values of porosity the temperature difference will become constant at a particular CL/EL ratio it is taken as 2.4 from the Fig 3.

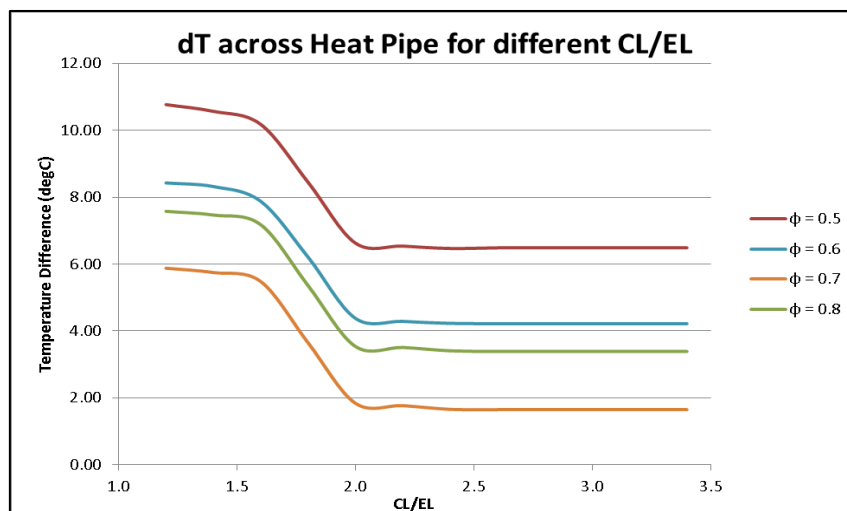


Fig 3: Comparing Results for Varying Porosity.

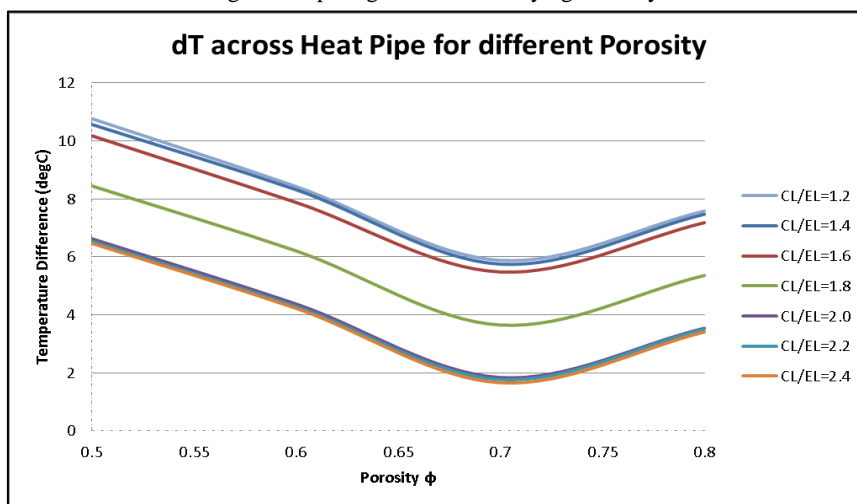


Fig 4: Comparing Results for Varying CL/EL ratio.

Fig 4 shows, the different curves which are obtained due to temperature difference in the heat pipe for various CL/EL ratio. It is observed from the above figures, for the entire CL/EL ratio the temperature difference reaches minimum value at a certain value of porosity. That value of the porosity is porosity value on which the maximum heat transfer can occur.

From both the Figure the CL/EL ratio and the porosity of the heat pipe at which maximum heat transfer can take place is optimized.

4. CONCLUSION

CFD analysis of heat pipe has been carried out with Ansys CFX. Optimization study of condenser length and porosity has been carried out. It is found that Condenser to Evaporator length ratio more than 2.4 will not affect the heat pipe performance. Optimization study on different porosities is also performed. It is found that wick porosity of 0.7 gives a better performance. Lower porosity helps in better capillary effect but reduces the flow which eventually leads to drying up of evaporator. Higher porosity aids liquid flow through pores but capillary effects will be less which again results in the flooding of Condenser.

REFERENCE

1. Nouri-Borujerdi and M. Layeghi, "A Numerical Analysis of Vapor Flow in Concentric Annular Heat Pipes", ASME, Vol. 126, pp. 442-448, May 2004.
2. Faghri and S. Thomas, "Performance Characteristics of a Concentric Annular Heat Pipe: Part I- Experimental Prediction and Analysis of the Capillary Limit", Transaction of ASME: Journal of Heat Transfer, Vol. 111, pp. 844-850, 1989.
3. Ali Mahtabroshan and Shoeib Mahjoub, "Numerical Simulation of a Conventional Heat Pipe", World Academy of Science, Engineering and Technology, Vol. 2, pp. 117-122, 2008.
4. Banjerd Saengchandr and Nitin V Afzulpurkar, "A Novel Approach for Cooling Electronics Using a Combined Heat Pipe and Thermoelectric Module", American J. of Engineering and Applied Sciences 2, pp. 603-610, 2009.
5. Somasundaram, A. Mani and M. Kamaraj, "Numerical Analysis of Thermal Performance of Flat Heat Pipe", International Refrigeration and Air Conditioning Conference, pp.1-10, 2012D. L. Davids, "Recovery Effects in Binary Aluminum Alloys", Ph.D. Thesis, Harvard University, 1998.